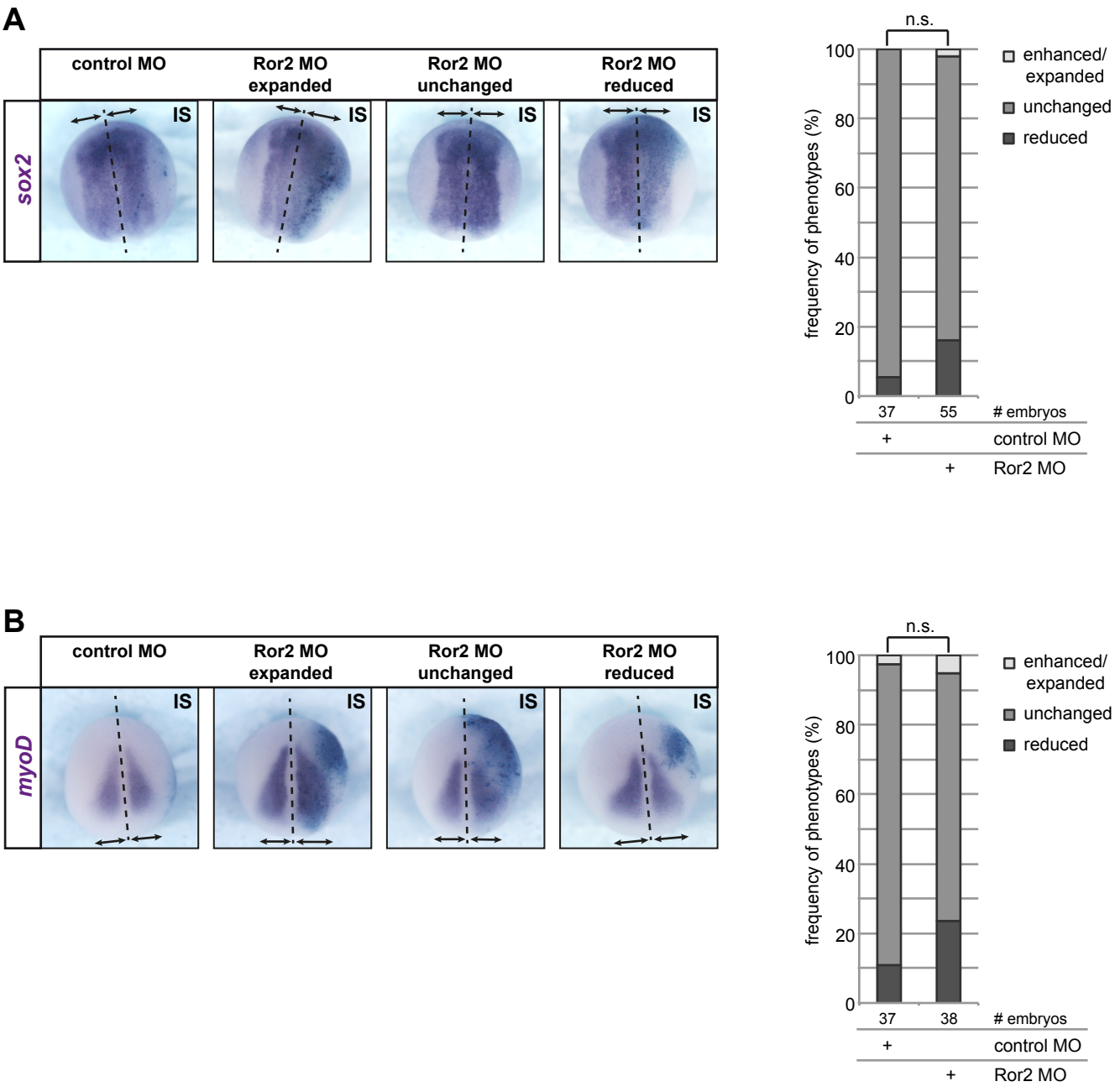

Supplementary Figure 1. Ror2 knock-down in the ectoderm did not affect mesoderm or neural induction.

Images show representative examples of embryos injected in one dorso-animal blastomere at the eight-cell-stage as indicated; the IS is oriented to the right. The neural plate was visualized by in situ hybridization using a *sox2* probe (Mizuseki et al. 1998), the paraxial mesoderm by *myoD* (Rupp et al. 1994). At least three independent experiments are summarized in the graphs. Statistically significant differences according to the $\chi 2$ test are indicated by "§" (§§<0.01, §<0.05, n.s. not significant). The total number of embryos is indicated below each column.
(A) Ror2 MO injection did not affect neural induction as judged by in situ hybridization against *sox2*. (B) Mesoderm induction (*myoD*) was also normal in Ror2 morphant embryos and did not differ significantly from controls.

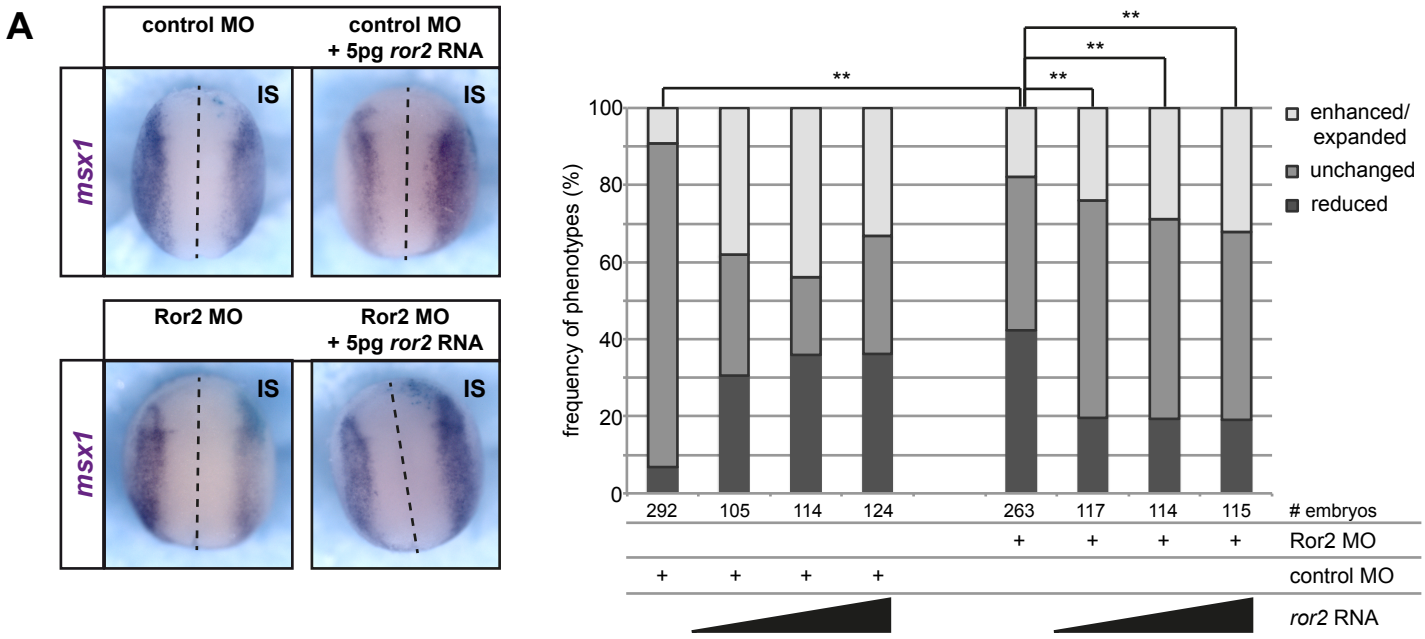

Supplementary Figure 2. Co-injection of Ror2 MO with a MO-insensitive *ror2* mRNA restores *msx1* expression.

Increasing doses (5pg to 30 pg) of MO-insensitive *ror2* RNA were co-injected with control 5MM MO or Ror2 MO. Images show representative examples of embryos injected as indicated and probed for *msx1* mRNA. Frequencies of the observed phenotypes from three independent experiments are summarized in the graph and the total number of embryos analyzed is indicated below the respective columns. Two-sample Wilcoxon rank sum test was performed to determine differences between experimental groups. Asterisks indicate statistically significant differences (** p-value < 0.01, n.s.=not significant).

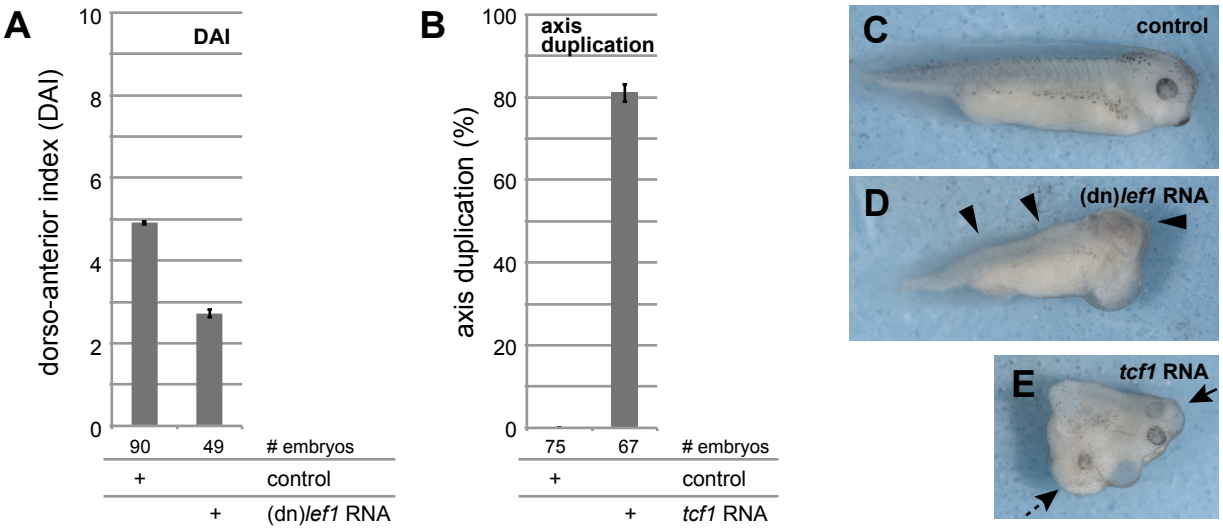

Supplementary Figure 3. Inhibition and activation of Wnt/β-Catenin signaling by dnLEF and TCF1 respectively.

(A) (dn)*lef1* RNA (Behrens et al. 1996) was injected in both dorsal blastomeres of four-cell-stage embryos, embryos were cultured till NF stage 37 and scored for the presence of dorsal and anterior structures according to (Kao et al. 1988). The average dorso-anterior index (DAI) was calculated and plotted in the graph (average ± SD). (B) *tcf1* RNA was injected in both ventral blastomeres of four-cell-stage embryos, embryos were cultured till NF stage 37 and scored for the presence of a secondary body axis (McMahon et al. 1989). The percentage of axis duplication is plotted in the graph (average ± SD). Representative images of embryos are shown in (C) control embryo, (D) (dn)*lef1* RNA injected embryo and (E) *tcf1* RNA injected embryo.

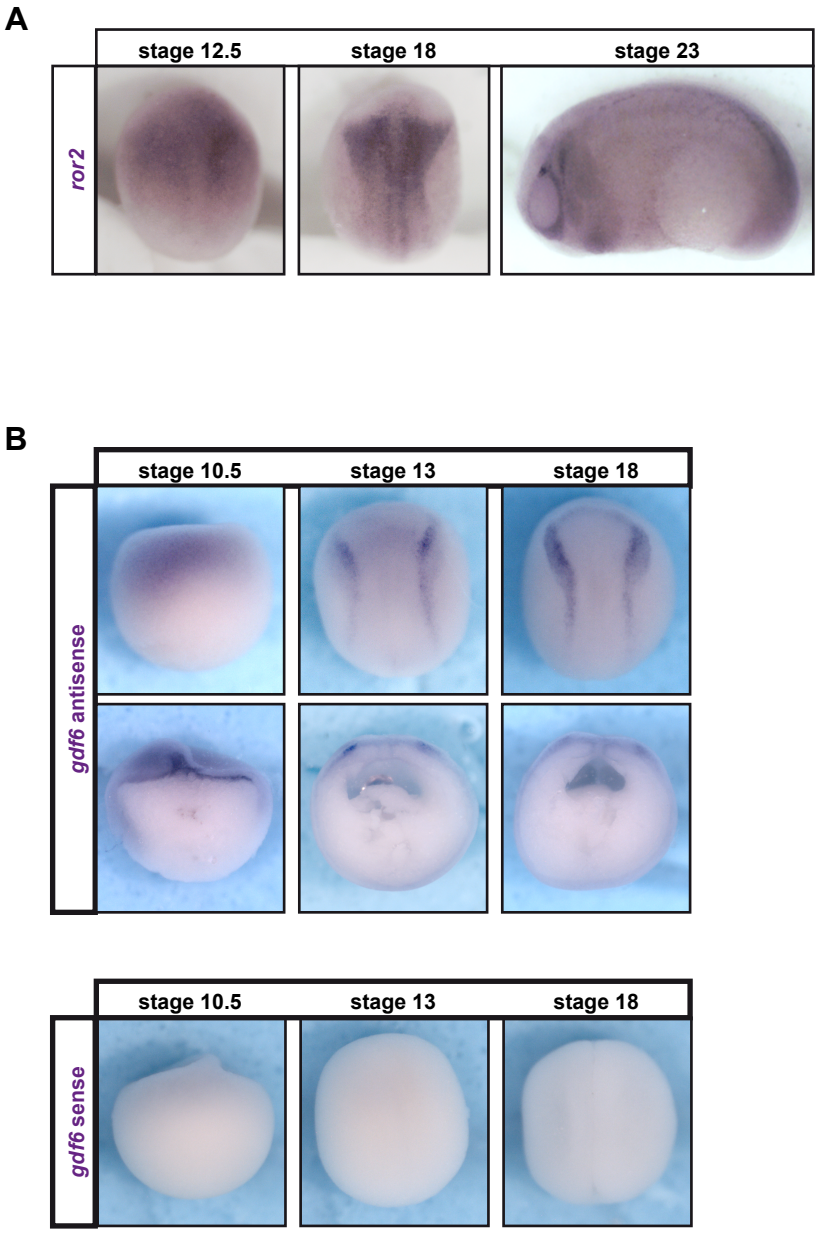

Supplementary Figure 4. Expression patterns of *ror2* and *gdf6*.

(A) Whole-mount in situ hybridization of uninjected albino embryos at NF stage 12.5, 18 and 23 shows expression of *ror2* in the neuroectoderm at stage 12.5, and in the pre-migratory and migrating neural crest at stages 18 and 23.
(B) At NF stage 10.5, 13 and 18 *gdf6* is expressed in the animal ectoderm at stage 10.5, at the neural plate border at stage 13 and in the pre-migratory neural crest at stage 18. Bi-sectioned embryos confirm expression in the ectoderm and hybridization with a sense probe the specificity of the signal.

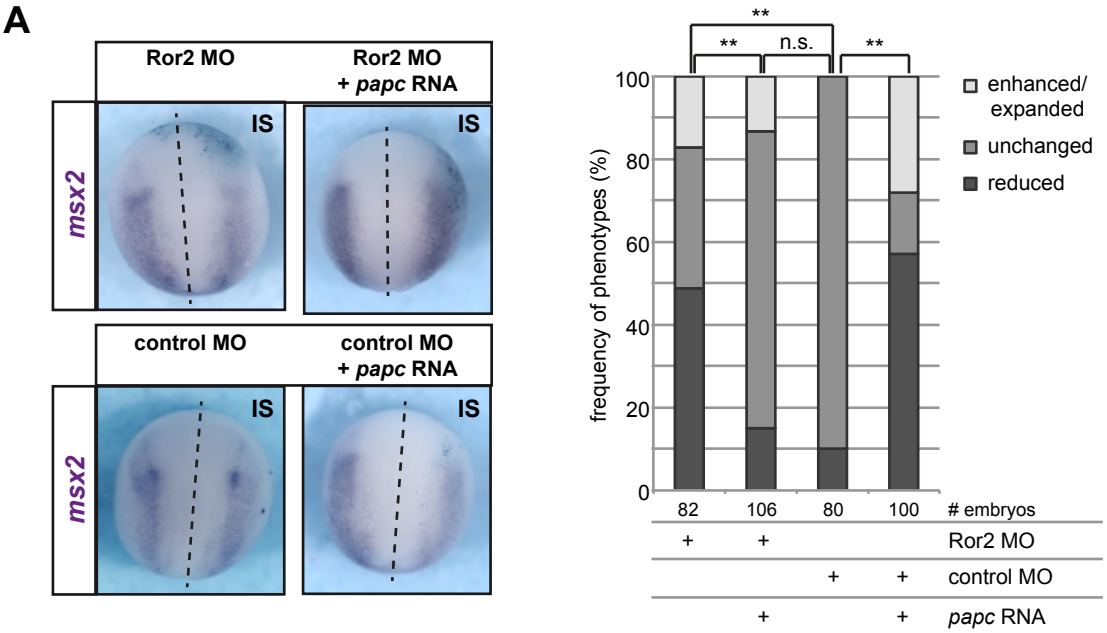

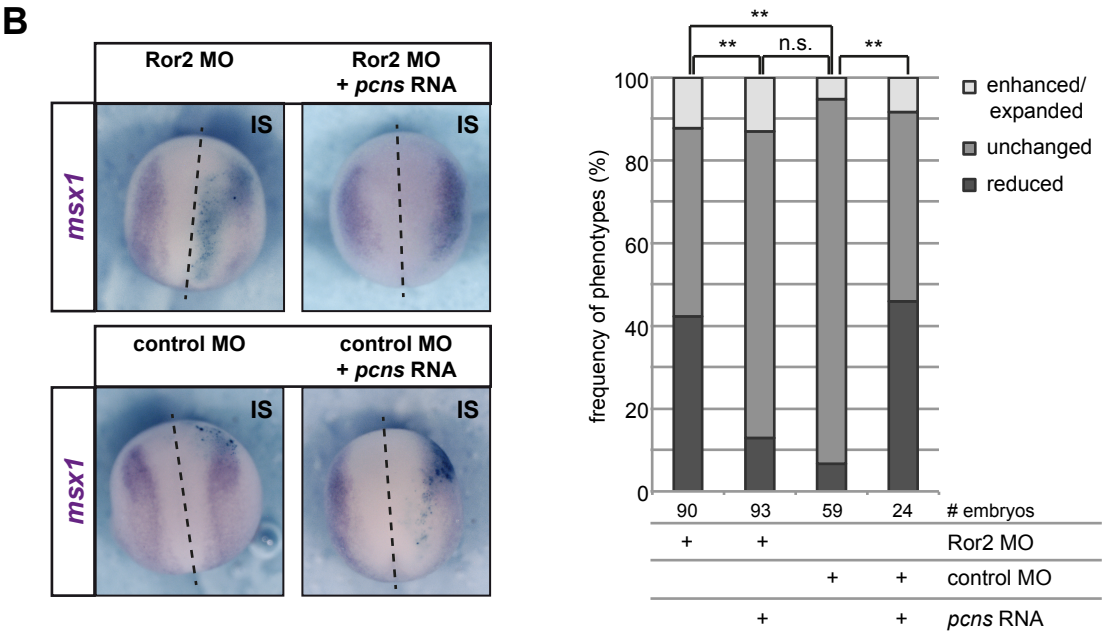

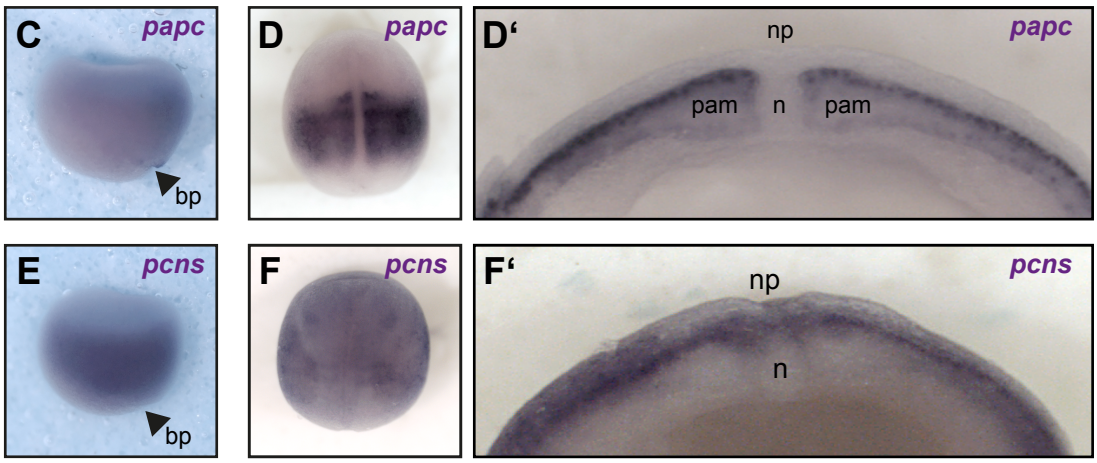

Supplementary Figure 5. Ror2 signals via a beta-catenin independent pathway in neural plate border specification.

Ror2 antisense morpholino (Ror2 MO) or control MO (5MM) was co-injected with synthetic mRNA encoding for PAPC or PCNS and a *lacZ* plasmid as lineage tracer into one dorso-animal blastomere of 8-cell stage embryos. Two sample Wilcoxon rank sum test was performed to determine differences between experimental groups Asterisks indicate statistically significant differences (**<0.01, *<0.05, n.s.=not significant).
(A) Overexpression of PAPC rescued *msx2* expression. Images show representative embryos injected as indicated; the injected side is oriented to the right. Frequencies of the observed phenotypes from three independent experiments are summarized in the graph and the total number of embryos analyzed is indicated below the respective columns.
(B) Overexpression of PCNS rescued *msx1* expression. Images show representative embryos injected as indicated; the injected side is oriented to the right. Frequencies of the observed phenotypes from three independent experiments are summarized in the graph and the total number of embryos analyzed is indicated below the respective columns.
(C)-(F) The expression pattern of *papc* and *pcns* in early and late gastrula stage embryos was determined by in situ hybridization. At stage 10.5 *papc* expression is limited to the dorsal blastopore lip (C). At stage 13 *papc* is expressed in the pre-somitic mesoderm (D). Expression is limited to the mesoderm and not detectable in the neural plate as visible in the cross-section (D'). *pcns* expression extends more laterally than *papc* at stage 10.5 (E); at stage 13 *pcns* is expressed in the ectoderm and in the first two forming somites (F). The cross-section (F') shows expression in the deep layer of the ectoderm.

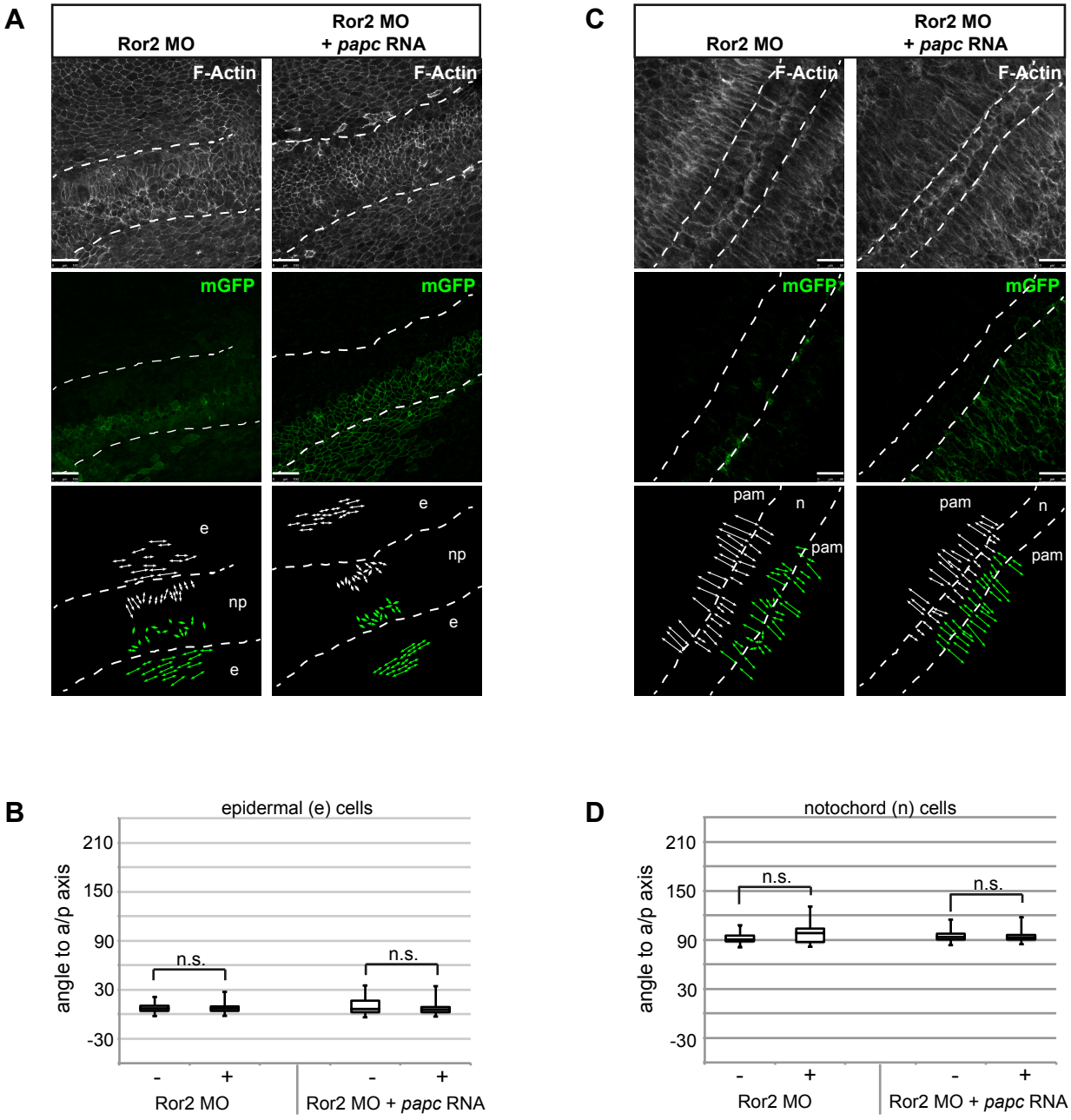

Supplementary Figure 6. Original images of neural plate explants.

Optical sections showing phalloidin staining and mGFP signal in explants injected as indicated. Green arrows indicate cell orientation on the injected side, white arrows show orientation on the uninjected side.
(A) Cell orientation in the neural plate. The prospective border between epidermis and neural plate is indicated by dashed lines. Orientation and position of epidermal (e) and neural plate (np) cells is illustrated in the schematic.
(B) Box plots illustrating the angle between long axes of individual epidermal cells and the anterior-posterior (a-p) axis in the epidermis. Epidermal cells are oriented parallel to the a-p axis; no significant difference was observed between cells on the injected side versus the non-injected side in Ror2 MO injected explants (n.s., two-sided separate variance t-test, p-value = 0.8186) or embryos co-injected with Ror2 MO and *papc* RNA (n.s., two-sided separate variance t-test, p-value = 0.1434).
(C) Cell orientation in the mesoderm of explants injected as indicated. Orientation and position of paraxial mesoderm (pam) and notochord (n) cells is illustrated in the schematic. Dashed lines indicate the position of the notochord.
(D) Box plots illustrating the angle between long axes of individual notochord cells and the anterior-posterior (a-p) axis in the notochord. Notochord cells are oriented perpendicular to the a-p axis; no significant difference was observed between cells on the injected side versus the non-injected side in Ror2 MO injected explants (n.s., two-sided separate variance t-test, p-value = 0.2110) or embryos co-injected with Ror2 MO and *papc* RNA (n.s., two-sided separate variance t-test, p-value = 0.3738).

Supplementary Materials and Methods

Supplementary Table 1
Primer sequences for RT-PCR and qPCR

Primer name	Sequence	Reference
qPCR		
bmpr1a_fwd	gttggttccgtgaaactgaaatc	Schille et al. 2016
bmpr1a_rev	aatccacaagctgcagaataagc	Schille et al. 2016
bmpr1b_fwd	ttggtacctagcgacccatctta	Schille et al. 2016
bmpr1b_rev	ctctgtcatgagctttcccatct	Schille et al. 2016
gdf6_fwd	gcccaccaaattgactcctatc	
gdf6_rev	tggcacaccaactgctacctac	
papc_fwd	cccagtcggtctcttcttctttg	Schambony and Wedlich 2007
papc_rev	ttgctgatgctgctcttggttag	Schambony and Wedlich 2007
pcns_fwd	ggactcagacactgaccataacg	
pcns_rev	tgagcacgagttgagagtctagg	
odc_fwd	cattgcagagcctgggagata	Schambony and Wedlich 2007
odc_rev	tccactttgctcattcaccataac	Schambony and Wedlich 2007
sox8_fwd	gccttatgctacacccatcctc	
sox8_rev	agaatttcagccaccagagacc	
msx2_fwd	tctcaccttccccaacaagaa	
msx2_rev	tggagaactctgccctctctg	
RT-PCR		
odc_fwd	gatgggctggatcgtatcgt	
odc_rev	tggcagcagtacagacagca	
bra_fwd	ttcagcctgtctgtcaatgc	
bra_rev	tttgtgctccatgctcatacaa	
chd_fwd	cctccaatccaagactccagcag	Schille et al. 2016
chd_rev	ggaggaggaggagctttgggacaag	Schille et al. 2016
epid. cytokeratin_fwd	aggtctgacatggaacaccaga	
epid. cytokeratin_rev	cgcattctgttggatttactcg	
ror2_fwd	tcctgctagaagaccaagat	
ror2_rev	aggtttgggtatgatctgag	
papc_fwd	cacacatctggttggcacct	
papc_rev	cttgttgattcggtggctga	
msx2_fwd	tctcaccttccccaacaagaa	
msx2_rev	tggagaactctgccctctctg	

Supplementary Table 2
Probes for in situ hybridization

probe	Reference
twist	(Hopwood et al., 1989)
snail2	(Mayor et al., 1995)
c-myc	(Bellmeyer et al., 2003)
ap2α	(Winning et al., 1991)
msx1	(Suzuki et al., 1997)
msx2	(Khadka et al., 2006)
gbx2	(Li et al., 2009)
zic1	(Nakata et al., 1998)
pax3	(Bang et al., 1999)
gdf6	(Chang and Hemmati-Brivanlou, 1999)
ror2	(Hikasa et al., 2002)
bmpr1a	(Schille et al., 2016)
bmpr1b	(Schille et al., 2016)
papc	(Kim et al., 1998)
pcns	(Rangarajan et al., 2006)

Expression plasmids

pCS2 Ror2-mCherry, pCS2-Gdf6, pCS2 PCNS, pCS2 TCF1 and pCS2 Dlv2ΔDIX (Gentzel et al., 2015) were obtained by cloning the respective cDNAs into the pCS2 vector (Rupp et al., 1994), pCS2 caBMPR has been generated by subcloning ca hBMPR1a (Varley et al., 1998) into the pCS2 vector; pCS2 dnLEF (Behrens et al., 1996) and pCS2 PAPC and pCS2 mGFP (Kim et al., 1998) have been kind gifts from J. Behrens and E. De Robertis respectively.

Image analysis

Whole-mount pSmad1,5,8 staining

Medio-lateral intensity profiles of pSmad1,5,8 staining were measured after image conversion to gray scale and linear contrast adjustment using the Image J software package.
Three profiles plus one baseline were measured per image at different positions along the anterior-posterior axis and three different embryos were analyzed per treatment were analyzed. Intensity profiles of each individual image were averaged and baseline subtracted. The baseline-subtracted profiles from triplicate embryos were aligned along the dorsal midline and adjusted to compensate deviations in embryo width and position in the images. Intensities were averaged and the resulting curves were smoothed using a moving average algorithm.

Neural plate explants

Analysis of cell orientation was based on gray scale images of Phalloidin staining. After background subtraction z-projections of 5 z-levels covering the region of interest were calculated using the Image J software package to ensure clear detection of cell borders. Images were inverted and gamma corrected (gamma 4.5) to improve identification of individual cells. The anterior-posterior axis was defined by the notochord and the center of the neural plate respectively. The angles of individual cells towards the anterior-posterior axis were measured and plotted.

Supplementary References

Bang, A. G., Papalopulu, N., Goulding, M. D. and Kintner, C. (1999). Expression of Pax-3 in the lateral neural plate is dependent on a Wnt-mediated signal from posterior nonaxial mesoderm. *Dev Biol* **212**, 366–380.

Behrens, J., Kries, von, J. P., Kühl, M., Bruhn, L., Wedlich, D., Grosschedl, R. and Birchmeier, W. (1996). Functional interaction of beta-catenin with the transcription factor LEF-1. *Nature* **382**, 638–642.

Bellmeyer, A., Krase, J., Lindgren, J. and LaBonne, C. (2003). The protooncogene c-myc is an essential regulator of neural crest formation in xenopus. *Dev Cell* **4**, 827–839.

Chang, C. and Hemmati-Brivanlou, A. (1999). Xenopus GDF6, a new antagonist of noggin and a partner of BMPs. *Development* **126**, 3347–3357.

Gentzel, M., Schille, C., Rauschenberger, V. and Schambony, A. (2015). Distinct functionality of dishevelled isoforms on Ca2+/calmodulin-dependent protein kinase 2 (CamKII) in Xenopus gastrulation. *Mol Biol Cell* **26**, 966–977.

Hikasa, H., Shibata, M., Hiratani, I. and Taira, M. (2002). The Xenopus receptor tyrosine kinase Xror2 modulates morphogenetic movements of the axial mesoderm and

neuroectoderm via Wnt signaling. *Development* **129**, 5227–5239.

Hopwood, N. D., Pluck, A. and Gurdon, J. B. (1989). A Xenopus mRNA related to Drosophila twist is expressed in response to induction in the mesoderm and the neural crest. *Cell* **59**, 893–903.

Kao, K. R. and Elinson, R. P. (1988). The entire mesodermal mantle behaves as Spemann's organizer in dorsoanterior enhanced Xenopus laevis embryos. *Dev Biol* **127**, 64–77.

Khadka, D., Luo, T. and Sargent, T. D. (2006). Msx1 and Msx2 have shared essential functions in neural crest but may be dispensable in epidermis and axis formation in Xenopus. *Int J Dev Biol* **50**, 499–502.

Kim, S. H., Yamamoto, A., Bouwmeester, T., Agius, E. and Robertis, E. M. (1998). The role of paraxial protocadherin in selective adhesion and cell movements of the mesoderm during Xenopus gastrulation. *Development* **125**, 4681–4690.

Li, B., Kuriyama, S., Moreno, M. and Mayor, R. (2009). The posteriorizing gene Gbx2 is a direct target of Wnt signalling and the earliest factor in neural crest induction. *Development* **136**, 3267–3278.

Mayor, R., Morgan, R. and Sargent, M. G. (1995). Induction of the prospective neural crest of Xenopus. *Development* **121**, 767–777.

McMahon, A. P. and Moon, R. T. (1989). Ectopic expression of the proto-oncogene int-1 in Xenopus embryos leads to duplication of the embryonic axis. *Cell* **58**, 1075–1084.

Mizuseki, K., Kishi, M., Matsui, M., Nakanishi, S. and Sasai, Y. (1998). Xenopus Zic-related-1 and Sox-2, two factors induced by chordin, have distinct activities in the initiation of neural induction. *Development* **125**, 579–587.

Nakata, K., Nagai, T., Aruga, J. and Mikoshiba, K. (1998). Xenopus Zic family and its role in neural and neural crest development. *Mech Dev* **75**, 43–51.

Rangarajan, J., Luo, T. and Sargent, T. D. (2006). PCNS: a novel protocadherin required for cranial neural crest migration and somite morphogenesis in Xenopus. *Dev Biol* **295**, 206–218.

Rupp, R. A., Snider, L. and Weintraub, H. (1994). Xenopus embryos regulate the nuclear localization of XMyoD. *Genes Dev* **8**, 1311–1323.

Schille, C., Heller, J. and Schambony, A. (2016). Differential requirement of bone morphogenetic protein receptors Ia (ALK3) and Ib (ALK6) in early embryonic patterning and neural crest development. *BMC Dev Biol* 1–17.

Suzuki, A., Ueno, N. and Hemmati-Brivanlou, A. (1997). Xenopus msx1 mediates epidermal induction and neural inhibition by BMP4. *Development* **124**, 3037–3044.

Varley, J. E., McPherson, C. E., Zou, H., Niswander, L. and Maxwell, G. D. (1998). Expression of a constitutively active type I BMP receptor using a retroviral vector promotes the development of adrenergic cells in neural crest cultures. *Dev Biol* **196**, 107–118.

Winning, R. S., Shea, L. J., Marcus, S. J. and Sargent, T. D. (1991). Developmental regulation of transcription factor AP-2 during Xenopus laevis embryogenesis. *Nucleic Acids Res* **19**, 3709–3714.